Available online at www.sciencedirect.com
SCIENCE DIRECT®
Electrochimica Acta 51 (2006) 1351–1358
ELECTROCHIMICA Acta
www.elsevier.com/locate/electacta

Synthesis and properties of imidazole-grafted hybrid inorganic–organic polymer membranes

Siwen Li [a], Zhen Zhou [a], Meilin Liu [a,*], Wen Li [b], Junzo Ukai [b], Kohei Hase [c], Masatsugu Nakanishi [c]

[a] *Center for Innovative Fuel Cell and Battery Technologies, School of Materials Science and Engineering, Georgia Institute of Technology, Atlanta, GA 30332-0245, USA*
[b] *Materials Engineering Department, Toyota Technical Center, USA, Inc., Ann Arbor, MI 48105, USA*
[c] *Material Engineering Division III, Vehicle Engineering Group, Toyota Motor Corporation, Susono, Shizuoka 410-1193, Japan*

Received 8 June 2005; received in revised form 2 July 2005; accepted 2 July 2005
Available online 15 August 2005

Abstract

Imidazole rings were grafted on alkoxysilane with a simple nucleophilic substitute reaction to form hybrid inorganic–organic polymers with imidazole rings. Proton exchange membranes (PEM) based on these hybrid inorganic–organic polymers and H_3PO_4 exhibit high proton conductivity and high thermal stability in an atmosphere of low relative humidity. The grafted imidazole rings improved the proton conductivity of the membranes in the high temperature range. It is found that the proton conductivities increase with H_3PO_4 content and temperature, reaching 3.2×10^{-3} S/cm at 110 °C in a dry atmosphere for a membrane with 1 mole of imidazole ring and 7 moles of H_3PO_4. The proton conductivity increases with relative humidity (RH) as well, reaching 4.3×10^{-2} S/cm at 110 °C when the RH is increased to about 20%. Thermogravimetric analysis (TGA) indicates that these membranes are thermally stable up to 250 °C in dry air, implying that they have a good potential to be used as the membranes for high-temperature PEM fuel cells.

Keywords: Proton exchange membranes (PEMs); Imidazole; Proton conductivity; Polymers; Phosphorus acid

1. Introduction

Proton electrolyte membranes (PEM) with high proton conductivity (>0.01 S/cm) but little or no dependence on humidity in the temperature range of 100–200 °C are critical to a new generation of PEM fuel cells with much higher energy efficiency and tolerance of anode catalyst to carbon monoxide poisoning [1,2]. The conventional perfluorosulfonic-polymers (such as Nafion®), however, have poor proton conductivity in low humidity and at high temperatures (above 80 °C), insufficient dimensional stability in different humidity, and high cost [3–9]. These limitations have stimulated the desire to develop other types of proton conducting membranes, including those with nanometer-sized hygroscopic metal oxides, polymer–H_3PO_4 membranes [2,9–13], and membranes based on hybrid inorganic–organic copolymers doped with proton-conductive inorganic compounds, such as $Zr(HPO_4)_2{\cdot}H_2O$ and $SiO_2{\cdot}12WO_3{\cdot}26H_2O$ [13–15]. Among all proton-conducting membranes developed in recent years, polybenzimidazole (PBI)–H_3PO_4 is the only one that has been commercially applied as electrolytes of fuel cells [16]. However, the proton conductivity of PBI–H_3PO_4 membranes is still humidity dependent, and the membrane is usually used in fuel cells operated at high current density [17]. Also, the mechanical properties degrade with the content of H_3PO_4 [11,13]. Thus, the development of new proton exchange membranes (PEMs) is still one of the critical challenges facing fuel cell technologies.

* Corresponding author. Tel.: +1 404 894 6114; fax: +1 404 894 9140.
E-mail address: meilin.liu@mse.gatech.edu (M. Liu).

0013-4686/$ – see front matter © 2005 Elsevier Ltd. All rights reserved.
doi:10.1016/j.electacta.2005.07.010

It has been reported that at least 98% of the total conductivity of pure H_3PO_4 originates from the structure diffusion of protons [17]. Phosphonic acid is an ideal proton conductor. Phosphosilicate gels, prepared from H_3PO_4 and tetraethyoxysilane (TEOS), have high proton conductivity above 100 °C in low humidity [14], but they are too brittle with little mechanical flexibility to be useful in practical electrochemical devices. As an attempt to improve the mechanical properties, 3-glycidoxypropyltrimethoxysilanes (GPTS) was introduced into silicate–H_3PO_4 gels as the former of hybrid inorganic–organic polymer network [18]. The obtained membranes have much better mechanical properties and can be easily made into membranes with a thickness of 20 μm supported on porous carbon boards. Because the organic chains of GPTS are short and tend to form three-dimensional polymer network, the GPTS-based self-standing membranes do not have enough flexibility for practical application as the electrolyte of PEM fuel cells.

The addition of heterocycles (such as imidazole and pyrazole), instead of water, to sulfonated polyetherketone and the oxo acids has promoted the proton transport process described by the Grotthuss-type mechanism (structure diffusion) [4,19]. For example, a mixture of benzimidazole with 10 mole% of H_3PO_4 has a conductivity of 0.05 S/cm at 200 °C [16]. Some polymer proton conductors doped with such heterocycles, mainly imidazole are reported to have high proton conductivity in anhydrous state [4,19,20]. However, for fuel cell application in an open environment, such heterocycles must be immobilized in the membranes to minimize instability due to possible evaporation. Imidazole ring was stabilized by copolymerization of vinylimidazole and vinylphosphonic acid, but the proton conductivity of the copolymer is very low (10^{-7} S/cm at 160 °C). This was attributed to the fact that imidazole rings were attached to the backbone too tightly that the local mobility of imidazole rings was limited [17,19,21].

Here, we report a new class of hybrid inorganic–organic polymers synthesized from bis(3-methyldimethyoxysilyl)polypropylene oxide (MDSPPO, see Scheme 1A), 1,4-bis(trimethoxysilylethyl)benzene (BTMSEB, see Scheme 1B). Bis(triethoxysilyl)octane (BTESO, see Scheme 1C) and tetraethyoxysilane. Because MDSPPO has a long polypropylene (PPO) chain ended with methyldimethoxysilyl groups, the formed two-dimensional hybrid inorganic–organic copolymer network is highly flexible. TEOS, BTESO and BTMSEB were used as a cross-linker to improve the mechanical strength. Meanwhile, imidazole rings were grafted on the hybrid inorganic–organic copolymer backbone through a short soft organic chain to ensure enough local mobility of the imidazole rings. The ideal molecular structure of the hybrid inorganic–organic membranes and the proton transport between imidazole rings and H_3PO_4 molecules are schematically shown in Fig. 1.

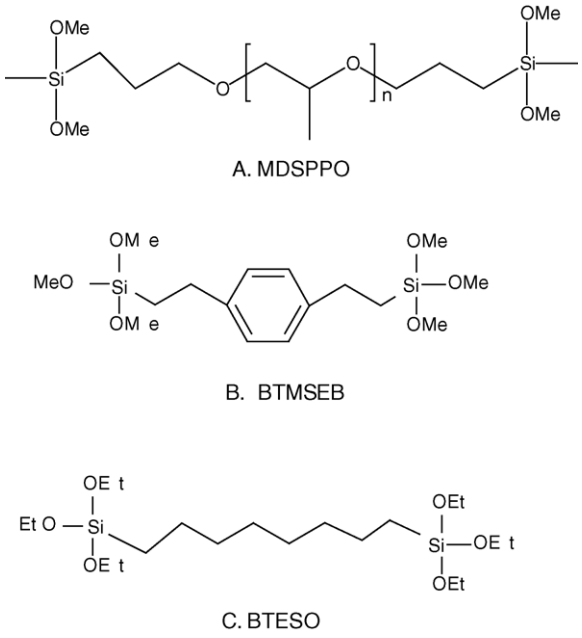

Scheme 1. Molecule structures of precursors as network formers. (A) MDSPPO, (B) BTMSEB, (C) BTESO.

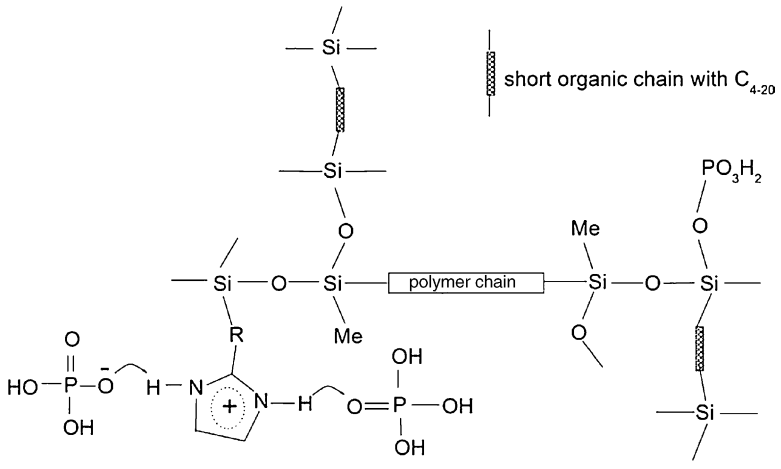

Fig. 1. Ideal molecule structure of a new hybrid inorganic–organic copolymer grafted with imidazole rings.

The new membranes showed high proton conductivity in environments of low relative humidity, high thermal stability, good mechanical properties, and good water-resistance. They have great potential as PEM electrolytes in high-temperature PEM fuel cells and other electrochemical devices.

2. Experimental

2.1. Synthesis of 2-triethoxysilylpropylthiomethyl-1H-benzimidazole (BISSi, see Scheme 2)

1.9634 g 3-mercaptopropyltrimethoxysilane (10 mmole) was dissolved in 10 ml of anhydrous ethanol, mixed with 0.84 g of potassium ethoxide (10 mmole, 24% solution in ethyl alcohol), and then stirred for 10 min. 1.6661 g of 2-(chloromethyl)benzimidazole (10 mmole) in 20 ml was added dropwise to the above mixture and stirred for about 12 h. TLC was used to check if the reaction has been completed. The white precipitate KCl was removed by filtration. About 2.2 g of 2-triethoxysilylpropylthiomethyl-1H-benzimidazole was separated from the filtrate through a silicate gel column chromatography eluted with ethyl acetate and hexane (50/50 in volume) (60% yield). It is a yellow oil-like liquid. ^{1}H NMR in $CDCl_3$: δ = 10.80 (1H, brs), 7.17-7.66 (4H, m), 3.95 (2H, s), 3.75 (6H, m), 2.50 (2H, t, $J_{H–H}$ = 7.30), 1.65 (2H, m), 1.54 (9H, t, $J_{H–H}$ = 7.01), 0.65 (2H, t, $J_{H–H}$ = 8.18).

2.2. 2-[(p-Triethoxysilylethylphenylmethyl)thio]-1H-imidazole (ImSSi, see Scheme 3)

ImSSi was synthesized from 2-mercaptoimidazole and ((chloromethyl)phenylethyl)-trimethoxysilane with the same method. 1.0001 g of 2-mercaptoimidazole (10 mmole) was dissolved in 20 ml anhydrous ethanol and mixed with 0.84 g of potassium ethoxide (10 mmole, 24% solution in ethyl alcohol), and then stirred for 10 min. 2.7482 g of ((chloromethyl)phenylethyl)-trimethoxysilane (10 mmole) was added dropwise to the mixture, and then stirred for 6 h. The white precipitate KCl was removed by filtration. About 2.4 g of ImSSi was separated from the filtrate through a silicate gel column chromatography eluted with ethyl acetate and hexane (50/50 in volume) (yield 65%). It is a colorless viscous liquid. ^{1}H NMR in DMSO-d^6: δ = 12.20 (1H, bs), 7.11 (6H, m), 4.17 (2H, s), 3.76 (6 H, m), 2.56 (2H, m), 1.15 (9H, t, $J_{H–H}$ = 6.95), 0.84 (2H, m).

2.3. Synthesis of 2-((3-triethoxysilylpropyl)thio)-1H-Imidazole (ImSSib, see Scheme 4)

ImSSib was synthesized from 2-mercaptoimidazole and 3-iodopropyl trimethoxysilane with the same method. 1.0001 g of 2-mercaptoimidazole (10 mmole) was dissolved in 20 ml anhydrous ethanol and mixed with 0.84 g of potassium ethoxide (10 mmole, 24% solution in ethyl alcohol), and then stirred for 10 min. 2.9017 g of 3-iodopropyltrimethoxysilane (10 mmole) was added dropwise to the mixture, and then stirred for 12 h. The white precipitate KI was removed by filtration. About 2.1 g of ImSSib was separated from the filtrate through a silicate gel column chromatography eluted with ethyl acetate and hexane (50/50 in volume) (yield 78%). It is a colorless viscous liquid. ^{1}H NMR in DMSO-d^6: δ = 7.11 (2H, s), 3.80 (6H, m, $J_{H–H}$ = 6.97), 3.00 (2H, t, $J_{H–H}$ = 7.05), 1.73 (2H, m), 1.20 (9 H, t, $J_{H–H}$ = 6.96), 0.76 (2H, m).

2.4. Preparation of membranes

The obtained BISSi, ImSSi, or ImSSib was dissolved in ethanol together MDSPPO (MW 600–900, see Scheme 1), BTMSEB, BTESO), and TEOS. After stirring for 20 min, 0.5 N HCl aqueous solution was added dropwise to the precursor solution, and further stirred for at least 12 h. At last, H_3PO_4 was added dropwise, and the solution was stirred for another 1–2 h to form uniform sols. The samples were labeled by their mole composition as *x*M–*y*B (or O)–*z*T–*m*BISSi (ImSSi/ImSSib)–*n*P, where *x*, *y*, *z*, and *m* refer to the moles of Si in MDSPPO, BTMSEB (or BTESO), TEOS, and BISSi (or ImSSi/ImSSib), respectively, and *n* is the moles of H_3PO_4. In this study, *x* = 2, *y* = 0 or 2, *z* = 1–3, *m* = 1–3, and *n* = 0, 3, 4, 5, 6, and 7. The membranes were dried at 60 °C for 3 days, at 80 °C for 3 h, and then at 100 °C for 1 h to evaporate the organic solvents and water.

2.5. Characterizations

X-ray diffraction (XRD) patterns of the gels were obtained using a Philips PW 1800 diffractometer (with Cu Kα radiation). The morphologies and microstructures were characterized using a scanning electron microscope (SEM, Hitachi S-800). FT-IR spectra were recorded with a Bruker Equinox 55 spectrometer. Thermogravimetric analysis (TGA) and differential scanning calorimetry (DSC) of the samples in dry air were performed using a Rheometric Scientific STA 1500. ^{1}H NMR spetra were recorded on a Bruker AMX 300 spectrometer operating at 300 MHz. The status of phosphorous acid in the hybrid inorganic–organic membranes was studied using ^{31}P MAS NMR (a Bruker DSX 400 spectrometer operating at 161.86 MHz). The ^{31}P signal from $NH_4H_2PO_4$ at 298 K was referenced to δ = 0 ppm. The proton conductivities of the membranes were determined using an impedance analyzer (a SI 1255 frequency response analyzer and a SI 1286 potentiostate/galvanostate) in the frequency range of 0.01 Hz–5 MHz. Two silver pellets were used as the electrodes. The measurements were run in a small dry oven.

3. Results and discussion

3.1. Synthesis of imidazole ring grafted alkoxysilanes

The immobilization of imidazole rings through a nucleophilic substitute reaction between –C–X (X = Cl, Br or I)

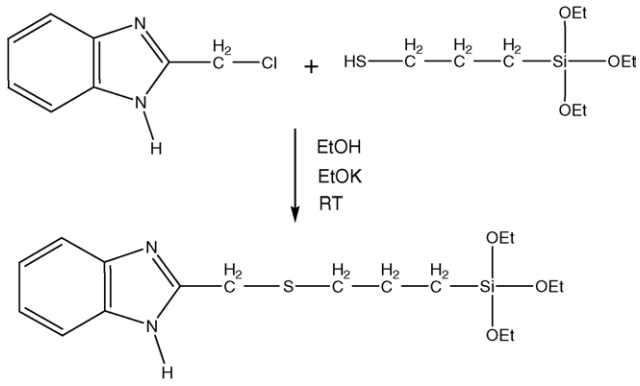

Scheme 2. Synthesis of 2-triethoxysilylpropylthiomethyl-1H-benzimidazole (BISSi).

and –SH is simple and effective [22,23]. The reactions have to be processed in anhydrous solvents and the separation process should be operated as quickly as possible to avoid hydrolysis of alkoxysilyl groups, which may reduce the yield through the silicate gel column. However, it is found that the conversion rate is almost 100% even at room temperature, and the reaction product can be used to make membranes without separation. Several months after we finished this work, we recognized a recent paper in which benzimidazole was attached on alkosilanes via a short organic chain through a two-step reaction [24]. Most recently, bezimidazole was grafted on polysiloxanes through a thiol-ene coupling reaction [25]. Compared with those works, our method is much simpler and more effective.

3.2. Proton conductivity of condensed organosilicon precursors with grafted imidazole

The hydrolyzed and condensed organosilicon precursors with grafted imidazole and benzimidazole as shown in Schemes 2 and 3 were ground and pressed into pellets. Deionized water was used for hydrolysis to avoid the

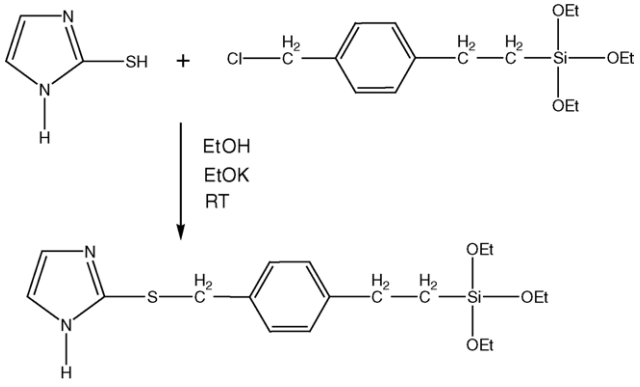

Scheme 3. Synthesis of 2-[(*p*-2-triethoxysilylethylenephenylenemethyl) thio]-1H-Imidazole (ImSSi).

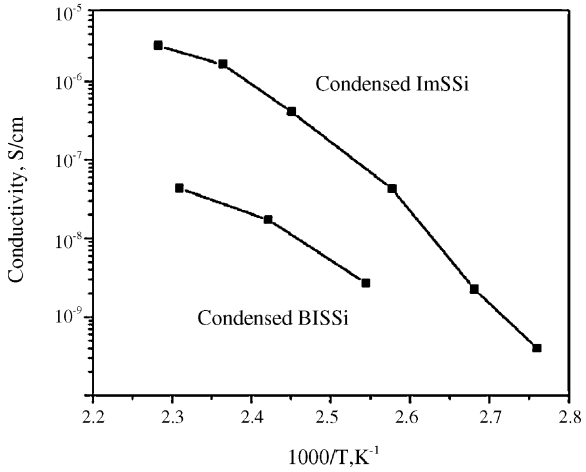

Fig. 2. Proton conductivity of condensed ImSSi and BISSi in anhydrous state.

introduction of extra H^+. The proton conductivities of the condensed ImSSi and BISSi were presented in Fig. 2. The proton conductivity of condensed ImSSi in anhydrous state is over 10^{-6} S/cm above 140 °C, comparable to the results obtained in the similar organosilicate with grafted imidazole [24,25]. It is believed that the proton conductivity originates from the proton transfer between imidazole rings, with the corresponding reorganization of the hydrogen bond pattern, following a Grotthuss-type mechanism [9]. The proton conductivities of the condensed BISSi are about two orders of magnitude smaller than those of the condensed ImSSI in the measured temperature range. The proton conductivity can be expressed by equation:

$$\sigma = ne\mu \quad (1)$$

where n is the concentration of protons, e is the electronic charge of protons, and μ is the mobility of protons. Comparatively, the concentration of proton defect originating from the self-dissociation of benzimidazole is larger than that of imidazole because benzimidazole has a smaller pK_a value than imidazole (pK_{BI} = 12.30, pK_{Im} = 14.52) [26,27]. However, the proton transport process involves the forming and breaking of hydrogen bonds through the rotation of heterocycle rings [9]. The local mobility of grafted benzimidazole ring should be much smaller than those of the grafted imidazole because the size of benzimidazole is much larger than the later one. So the proton mobility in the condensed BISSi is much smaller than that in the condensed ImSSi.

3.3. Appearance of hybrid inorganic–organic membranes

All membranes with compositions of 2M–(4x) T–xBISSi (ImSSi/ImSSib)–nP (x = 1, 2, and 3; n = 0, 3, 5, 7) and 2M–2B (or O)–1T–1BISSi–nP (n = 4, and 6) are highly flexible with good mechanical strength (see Fig. 3). The good

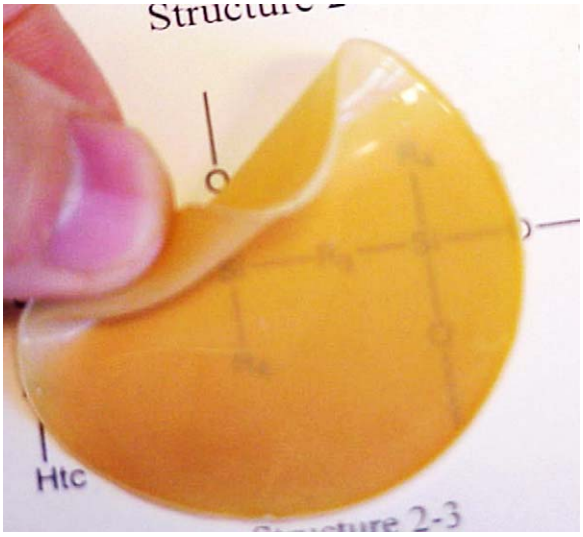

Fig. 3. Appearance of 2M–3T–1BISSi–5P. The membrane is highly flexible with good mechanical strength.

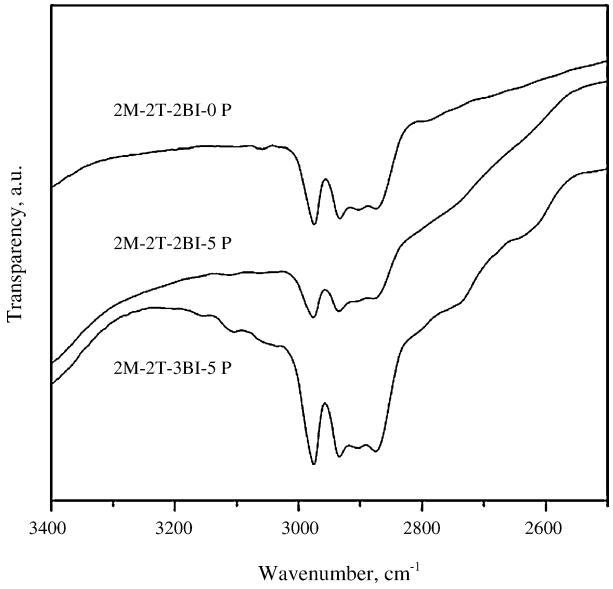

Fig. 4. FT-IR of 2M–*x*BISSi–*y*P ($x = 2$, $y = 0$, and 5; $x = 3$, $y = 5$).

mechanical properties originate from the unique molecule structures of the hybrid inorganic–organic copolymers as shown in Fig. 1. The three-dimensional –Si–O–Si– networks were connected by highly flexible polymer chains of polypropylene oxide through the Si–C bonds introduced by MDSPPO (see Scheme 1). The self-standing membranes with a thickness less than 0.1 mm can be readily cast with large size depending on the molds. A piece of membrane larger than 170 cm^2 was obtained using a glass dish as mold.

The new membranes keep un-deliquescent in ambient air for many days. When immersed in water at room temperature for 2 h, and then at 70 °C for 2 h, only about 30% of H_3PO_4 in the samples with compositions of 2M–2B–1T–1BISSi–6P and 2M–3T–1BISSi–5P leached out. For the sample without grafted imidazole rings, the membranes loss about 80% of H_3PO_4 under the same conditions. Except for the good affinity of Si–O network to H_3PO_4 and the hydrogen bonds between H_3PO_4 and PEO chains introduced by MDSPPO [14,28], the interaction between imidazole rings and H_3PO_4 may be the main reason of the high stability of H_3PO_4 in the membranes with grafted imidazole rings. The strong interaction between imidazole rings and H_3PO_4 was conformed by FT-IR spectrum of the membranes with grafted benzimidazole and H_3PO_4 in which a strong broad peak was observed from 2500 to 3200 cm^{-1} (see Fig. 4) [13,29]. The strong broad peak is from the hydrogen bond formed between NH groups on imidazole rings, $H_2PO_4^-$ and H_3PO_4 [29]. X-ray diffraction analysis suggested that all the membranes as obtained are amorphous. After heating in dry Ar from 100 to 140 °C for 6 h, no peak was observed in the XRD patterns, indicating that no crystallization took place between Si–O–Si network and H_3PO_4 as observed in inorganic Si–H_3PO_4 gels [14].

3.4. Status of H_3PO_4 in hybrid inorganic–organic membranes

Shown in Fig. 5 are the NMR spectra of two samples with composition of 2M–3T–1BISSi–3H_3PO_4 and 2M–2Oc–1T–1ImSSi–5P. Three ^{31}P resonance peaks were observed; one of which is too weak to be visible in the full spectrum. The main peak at $\delta = 0$ ppm is attributed to the undissociated H_3PO_4 and other dissociated species such as $H_4PO_4^+$ and $H_2PO_4^-$ [30,31]. The latter two species are known to be within 2 ppm of the undissociated H_3PO_4 signal [24]. The weak peaks at δ, −11 ppm and −24 ppm are due to the end unit of pyrophosphoric acid and tripolyphosphoric acid [15]. It should be mentioned that these weak peaks may be assigned to the phosphates bound to one or two silicon atoms through P–O–Si bonds, which means that H_3PO_4 was attached to the Si–O–Si network in the hybrid

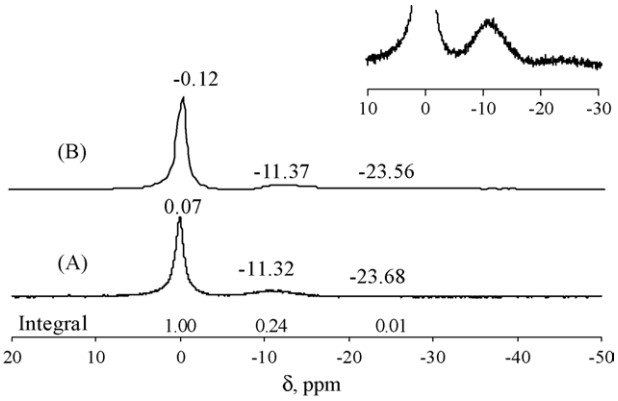

Fig. 5. ^{31}P NMR spectra of two hybrid inorganic–organic membranes with composition of (a) 2M–3T–1 BiSSi–3P and (b) 2M–2Oc–1T–1ImSSi–5P. Inset: spectra with magnification of intensity to show the weak peaks near −11.5 ppm and −23.68 ppm.

inorganic–organic copolymer [32,33]. The integral of the two weak peaks is about 20% of the total ^{31}P resonance peaks for the membrane, suggesting that about 20% of H_3PO_4 was grafted on the Si–O based hybrid inorganic–organic network and 80% of the phosphoric acid is present in the free form. Because the grafted imidazole and benzimidazole have strong interaction with H_3PO_4 molecules [13], the anion transference number in the new hybrid inorganic–organic polymer membranes should be smaller than that in pure H_3PO_4 ($t_{anion} = 0.02$) [17], implying that the ionic transport in the membrane is dominated by proton motion.

3.5. Thermal and chemical stability of hybrid inorganic–organic membranes

The thermal stability of all membranes was studied using TGA. Fig. 6 shows the TGA curves of 2M–3T–1BISSi–*x*P ($n = 3$, 5, and 7), 2M–3T–5P, and 2M–2B–1T–1BISSi–6P from room temperature to 400 °C in dry air at a heating rate of 3 °C/min. For the membranes with compositions of 2M–3T–1BISSi–*n*P, the onset of decomposition temperature decreased with H_3PO_4 contents varying from about 230 to 220 °C, and to 190 °C for the membrane with H_3PO_4 content of $n = 3$, 5, and 7, respectively. This is most likely because the complexation of acid molecules to the hybrid inorganic–organic copolymer network corrodes and oxidizes the PPO-based polymer backbone [13]. The membranes without grafted imidazole have much lower decomposition temperature. As shown in Fig. 5, the onset of decomposition temperature of 2M–3T–5P is about 170 °C, about 50 °C lower than 2M–3T–1BISSi–5P. The copolymer backbone grafting imidazole rings has much better thermal stability owing to the strong basic nature of imidazole rings. The thermal stability of the membranes was improved by the addition of BTMSEB and BTESO. The onset of decomposition temperature of the membranes was increased from 190 to 250 °C with the addition of BTMSEB and BTESO.

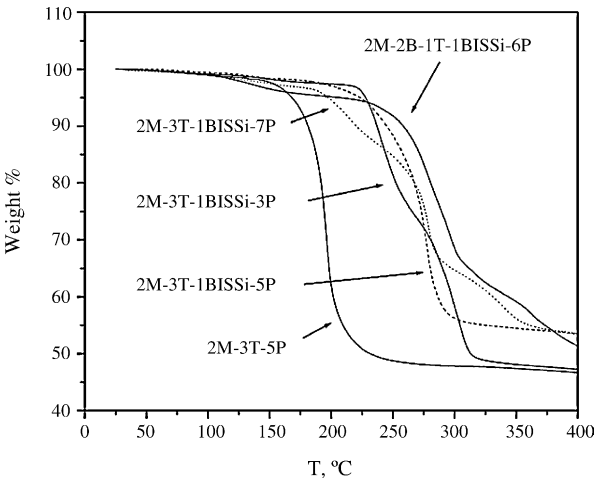

Fig. 6. TGA curves for several membranes measured in dry air at a heating rate of 5 °C/min.

The chemical stability was examined by immersing a piece of sample (0.5 cm × 2 cm) in a standard Fenton reagent (3% H_2O_2 aqueous solution with 2 ppm $FeSO_4$) at 80 °C [34]. It was found that the samples with a composition of 2M–2T–2BISSi–5P or 2M–2T–2ImSSi–5P were stable (no dissolution, no cracking, and no visible changes in mechanical flexibility and strength) after immersion in the solution at 80 °C for 24 h, suggesting that the new membranes have good chemical stability for fuel cell applications.

3.6. Proton conductivity of hybrid inorganic–organic membranes

Shown in Fig. 7 are the proton conductivities of membranes with various compositions. All the membranes were dried in dry Ar at 60 °C for 6 h, 80 °C for 3 h, and 100 °C for 2 h before proton conductivity measurements. Also, pro-

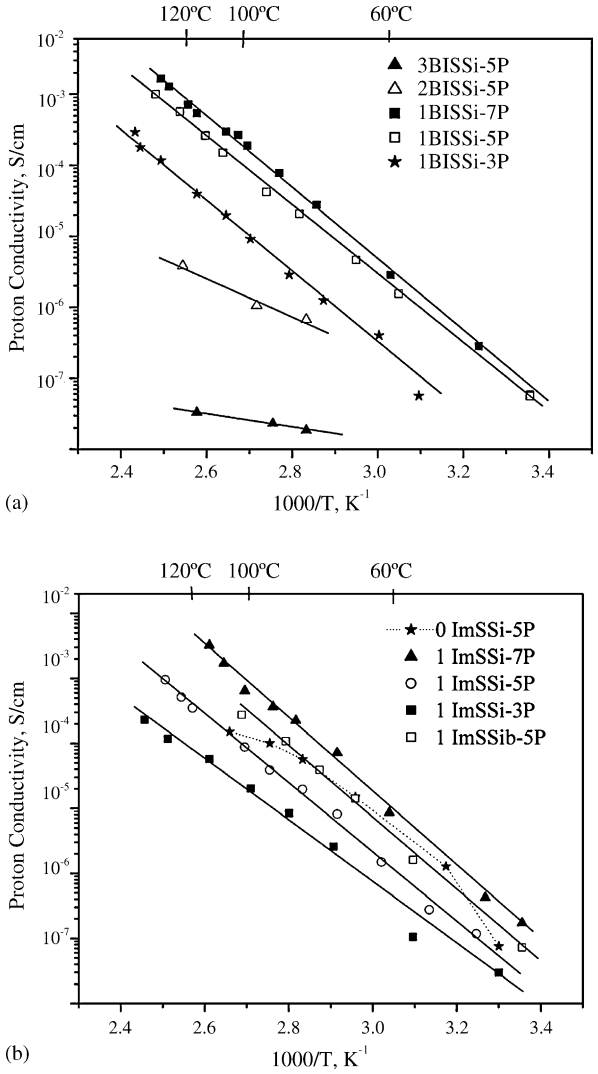

Fig. 7. Proton conductivity of (a) 2M–3T–*x*BISSi–*y*P ($x = 1$, $y = 3$, 5, and 7; and $x = 2$, and 3, $y = 5$) and (b) 2M–3T–*x*ImSSi–*y*P ($x = 0$, $y = 5$; $x = 1$, $y = 3$, 5, and 7) in anhydrous state.

ton conductivities were measured under anhydrous condition after samples were kept in dry argon for at least 2 h at each temperature. For all membranes studied, the proton conductivity increased with H_3PO_4 contents and with temperature. It is 3.2×10^{-3} S/cm at 110 °C for sample with a composition of 2M–3T–1ImSSi–7P. It was reported that PBI–6H_3PO_4 has a proton conductivity of 3.0×10^{-3} S/cm at 110 °C in anhydrous state [35]. The new membranes have similar proton conductivity with PBI–H_3PO_4 membranes [13,35]. The increase in proton conductivity with H_3PO_4 contents in the new hybrid inorganic–organic copolymer membranes is similar to other polymer–H_3PO_4 materials, indicating that the protons from H_3PO_4 self-dissociation are the main source of proton conductivity [9–13]. Comparing the imidazole-grafted membrane 2M–3T–1ImSSi–5P and 2M–3T–1ImSSib–5P to that with a composition of 2M–3T–5P, we can find that the proton conductivity of the imidazole-grafted membranes is smaller in lower temperature range, but obviously larger in high temperature range. It has been found that the viscosity of H_3PO_4–Imidazole systems, such as PBI–H_3PO_4–imidazole, has a dominating influence on the conductivity [35]. In the new membranes with grafted imidazole rings and H_3PO_4, the local mobility of the imidazole rings was depressed because of the high viscosity of the hybrid inorganic–organic polymer network and H_3PO_4 dispersed among the polymers. With increasing temperature, the local mobility of imidazole rings was released and increased the proton conductivity of the membranes. It is notable that the proton conductivity of the membrane with a composition of 2M–3T–1ImSSib–5P is much higher than that of membrane with a composition of 2M–3T–1ImSSi–5P. Comparing the molecule structures of ImSSi and ImSSib (see Schemes 2 and 3), it can be found that the organic chains that connect imidazole rings with Si are much different. The chain in ImSSib is much more flexible than that in ImSSi because there is a benz-ring in the chain of ImSSi. So the local mobility of imidazole rings in the membrane with ImSSib is higher than that with ImSSi. The flexible chain allows for the rapid transport of proton via structure diffusion (Grotthuss mechanism) [19], and hence the membranes with ImSSib have higher proton conductivity. The difference in morphology may influence the proton conductivity as well. The membranes with more flexible sidechains may have larger domains in which liquid H_3PO_4 formed passways for proton transport [13]. With increasing benzimidazole or imidazole contents, the proton conductivity of the membranes decreased (see Fig. 7 a). Because of the high viscosity of hybrid inorganic–organic polymer–H_3PO_4 systems, the local mobility of the grafted imidazole rings was highly limited. H_3PO_4 protonated imidazole rings and formed N–H^+ groups. The proton transport rate between N–H^+ and $H_2PO_4^-$ or among N–H^+ groups is much lower than that between H_3PO_4 and $H_2PO_4^-$, and thus the proton conductivity of the membranes decreased [17,36].

It appears that the membranes with BISSi display an Arrhenius-type behavior while the membranes with ImSSi and ImSSib show some visible deviation from Arrhenius-type behavior. The average activation energy of the membranes with compositions of 2M–3T–1ImSSi–*x*P ($x = 3$, 5, and 7) is about 0.91 eV, and that of the membranes with compositions of 2M–3T–1ImSSi–*x*P ($x = 3$, 5, and 7) is about 1.28 eV. However, the $\log \sigma$–T^{-1} curves of the membrane without imidazole rings, e.g. 2M–3T–5P, shows the character of Vogel–Tamman–Fucher (VTF) behaviors [3]. The different temperature dependence of proton conductivity for the membranes with imidazole rings is due possibly to different proton transport mechanism caused by the changes in viscosity, molecule structures and interaction between imidazole rings and H_3PO_4. In fact, the proton transport mechanism in the new membranes is very complex. The hydrogen defects in the new membranes originate from the dissociations among H_3PO_4 molecules and between H_3PO_4 molecules and imidazole rings grafted on the hybrid inorganic–organic copolymer network. Thus, the proton transport process includes the proton transport along the acid-imidazole ring-acid path and along the acid–acid path [36]. Meanwhile, the PPO organic chains (see Scheme 4) can also function as a good proton acceptor in addition to being a network former in the membranes [28].

To determine the dependence of proton conductivity on humidity of the new membranes, the proton conductivities of several samples were measured in the vapor of a saturated $MgCl_2$ aqueous solution from 70 to 120 °C. The calculated relative humidity in the closed chamber with saturated $MgCl_2$ aqueous solution is 26% at 70 °C, about 22.5% at 100 °C, and about 15% at 120 °C [37]. The samples were kept, at each temperature, for several hours until the measured proton conductivity became stable. Shown in Fig. 8 are the proton conductivities of samples with composition of 2M–2O (or B)–1T–1BISSi–*n*P ($n = 4$ and 6) with the calculated relative humidity. The proton conductivities of all samples are greater than 0.01 S/cm above 100 °C. It is about 0.04 S/cm at 110 °C for the sample with composition of 2M–2O–1T–1BISSi–6P.

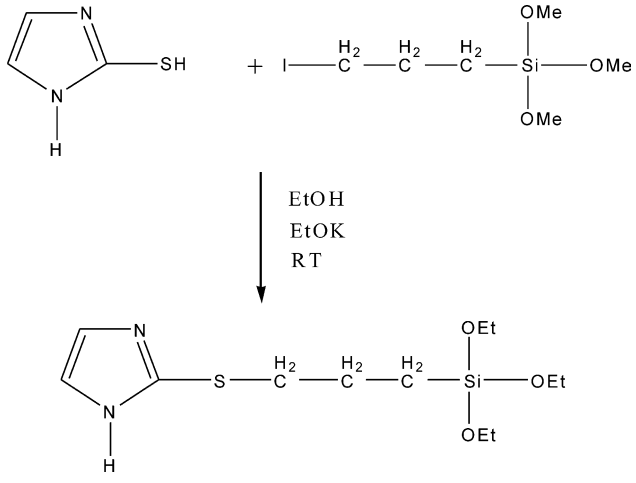

Scheme 4. Synthesis of 2-((3-triethoxysilylpropyl)thio)-1H-Imidazole (ImSSib).

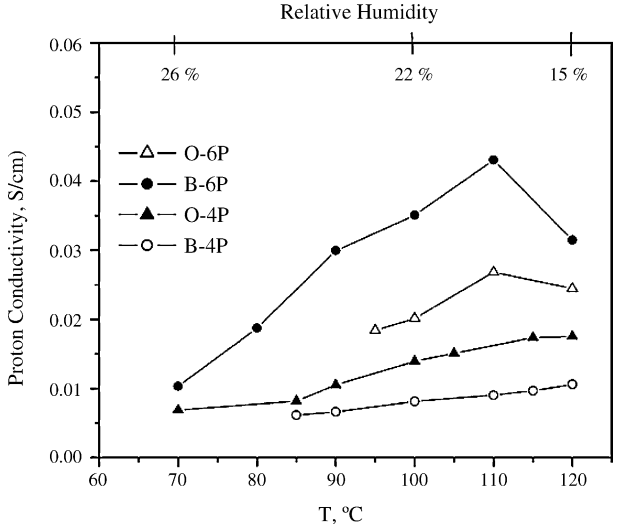

Fig. 8. Proton conductivity stability of 2M–2O (or B)–1T–1BISSi–*x*P (*x* = 3, 5, and 7) in the vapor of saturated $MgCl_2$ aqueous solution.

The much higher proton conductivity under wet conditions can be attributed to the higher mobility of H_3O^+ as a vehicle of proton [38]. It should be mentioned that no change in shape, color and conductivity of these membranes was observed after they were kept in the wet environments at 120 °C for more than 10 h.

4. Conclusion

In summary, a class of new membranes based on hybrid inorganic–organic polymer network and H_3PO_4 were synthesized. Imidazole rings have been successfully grafted on the hybrid inorganic–organic network through a short organic branch by simple and effective nucleophilic substitution reactions. The local mobility of the imidazole rings grafted on the hybrid inorganic–organic polymers is greatly affected by the viscosity of the membranes, the softness of the connecting chains, the flexibility of the backbones, and other factors. The improvement of proton conductivity depends critically on the molecule structures of the membranes. The new membranes based on the polymers with imidazole ring terminated side chains and H_3PO_4 have good mechanical properties and thermal stability up to 250 °C. The proton conductivity in environments of low relative humidity is relatively high, greater than 10^{-2} S/cm in an atmosphere with relative humidity about 20% at 100 °C. They have good potential for application in high-temperature PEM fuel cells and other electrochemical devices.

References

[1] P.L. Antonucci, A.S. Arico, P. Creti, E. Ramunni, V. Antonucci, Solid State Ionics 125 (1999) 431.
[2] M. Watanabe, H. Uchida, M. Emori, J. Phys. Chem. B 102 (1998) 3129.
[3] L. Depre, M. Ingram, C. Poinsignon, M. Popall, Electrochim. Acta 45 (2000) 1377.
[4] K.D. Kreuer, J. Membrane Sci. 185 (2001) 29.
[5] J.M. bae, I. Honma, M. Murata, T. Yamamoto, M. Rikukawa, N. Ogata, Solid State Ionics 147 (2002) 189.
[6] N. Chen, L. Hong, Solid State Ionics 146 (2002) 377.
[7] S. Surampudi, S.R. Narayanan, E. Vamos, H. Frank, G. Halpert, A. LaConti, J. Kosek, G.K. Prakash, G.A. Olah, J. Power Sources 47 (1994) 377.
[8] A.J. Appleby, F.R. Foulkes (Eds.), Fuel Cell Handbook, Krieger, Malabar, FL, 1993.
[9] K. Tsuruhara, M. Rikukawa, K. Sanui, N. Ogata, Y. Nagasaki, M. Kato, Electrochim. Acta 45 (2000) 1391.
[10] H. Wang, B.A. Holmberg, L. Huang, Z. Wang, A. Mitra, J.M. Norbeck, Y. Yan, J. Mater. Chem. 12 (2002) 834.
[11] J.S. Wainright, J.-T. Wang, D. Weng, R.F. Savinell, M. Lit., J. Electrochem. Soc. 142 (1995) L121.
[12] A. Schechter, R. Savinell, Solid State Ionics 147 (2002) 181.
[13] M. Rikukawa, K. Sanui, Prog. Polym. Sci. 25 (2000) 1463.
[14] A. Matsuda, T. Kanzaki, Y. Yoshinori, M. Tatsuminago, T. Minami, Solid State Ionics 139 (2001) 113.
[15] K. Hirata, A. Matsuda, T. Hirata, M. Tatsumisago, T. Minami, J. Sol–Gel Sci. Technol. 17 (2000) 61.
[16] Q. Li, R. He, J.O. Jensen, N.J. Bjerrum, Chem. Mater. 15 (2003) 4896.
[17] A. Bozkurt, W.H. Meyer, Solid State Ionics 138 (2001) 259.
[18] S. Li, M. Liu, Electrochim. Acta 28 (2003) 4271.
[19] M. Schuster, W.H. Meyer, G. Wegner, H.G. Herz, M. Ise, K.D. Kreuer, J. Maier, Solid State Ionics 145 (2001) 85.
[20] J. Sun, L.R. Jordon, M. Forsyth, D.R. MacFarlane, Electrochim. Acta 46 (2001) 1703.
[21] A. Bozkurt, W.H. Meyer, J. Gutmann, G. Wegner, Solid State Ionics 164 (2003) 169.
[22] T. Hamaguchi, A. Takahashi, T. Kagamizono, A. Manaka, M. Sato, H. Osada, Bioorg. Med. Chem. Lett. 10 (2000) 2657.
[23] A.W. Lutz, US Patent, 3,499,001.
[24] H.G. Herz, K.D. Kreuer, J. Maier, G. Scharfenberger, M.F.H. Schuster, W.H. Meyer, Electrochim. Acta 48 (2003) 2165.
[25] J.C. Persson, P. Jannasch, Macromolecular 38 (2005) 3283.
[26] J.A. Dean, Handbook of Org. Chem., McGray-Hill Book Company, 1987, p. 8–2.
[27] G.R.A. Agliano Jr., R.C. Knowlton, L.D. Byers, J. Org. Chem. 54 (1989) 5247.
[28] J. Qiao, N. Yoshimoto, M. Morita, J. Power Sources 105 (2002) 45.
[29] X. Glipa, B. Bonnet, B. Mula, J. Jones, J. Roziere, J. Mater. Chem. 9 (1999) 3045.
[30] A. Matsuda, T. Kanzaki, M. Tatsuminago, T. Minami, Solid State Ionics 145 (2001) 161.
[31] S.H. Chung, Y. Wang, S.G. Greenbaum, W. Bzducha, G. Zukowska, W. Wieczorek, Electrochim. Acta 46 (2001) 1651.
[32] C. Fernandez-Lorenzo, L. Esquivias, P. Barboux, J. Maquet, F. Taulelle, J. Non-Cryst. Solids 176 (1994) 189.
[33] P. Kohli, G.J. Blanchard, Langmuir 16 (2000) 695.
[34] K. Miyatake, N. Asano, M. Watanabe, J. Polym. Sci.: A 41 (2003) 3901.
[35] A. Schechter, R.F. Savinell, Solid State Ionics 147 (2002) 181.
[36] Y.L. Ma, J.S. Wainright, M.H. Litt, R.F. Savinell, J. Electrochem. Soc. 151 (2004) A8.
[37] D.R. Lide, CRC Handbook of Chemistry and Physics, CRC Press, Boca Raton, FL, 1998, pp. 15–26.
[38] K.D. Kreuer, Chem. Mater. 8 (1996) 610.